

# We are IntechOpen, the world's leading publisher of Open Access books Built by scientists, for scientists

6,900

Open access books available

185,000

International authors and editors

200M

Downloads

Our authors are among the

154

Countries delivered to

TOP 1%

most cited scientists

12.2%

Contributors from top 500 universities



WEB OF SCIENCE™

Selection of our books indexed in the Book Citation Index  
in Web of Science™ Core Collection (BKCI)

Interested in publishing with us?  
Contact [book.department@intechopen.com](mailto:book.department@intechopen.com)

Numbers displayed above are based on latest data collected.  
For more information visit [www.intechopen.com](http://www.intechopen.com)



# Fatigue Assessment of Highway Bridges under Traffic Loading Using Microscopic Traffic Simulation

*Gengwen Zhao, Chung C. Fu, Yang Lu and Timothy Saad*

## Abstract

Fatigue is a common failure mode of steel bridges induced by truck traffic. Despite the deterioration caused by environmental factors, the increasing truck traffic volume and weight pose a premier threat to steel highway bridges. Given the uncertainties of the complicated traffic loading and the complexity of the bridge structure, fatigue evaluation based on field measurements under actual traffic flow is recommended. As the quality and the quantity of the available long-term traffic monitoring data and information have been improved, methodologies have been developed to obtain more realistic vehicular live load traffic. A case study of a steel interstate highway bridge using microscopic traffic simulation is presented herein. The knowledge of actual traffic loading may reduce the uncertainty involved in the evaluation of the load-carrying capacity, estimation of the rate of deterioration, and prediction of remaining fatigue life. This chapter demonstrates a systematic approach using traffic simulation and bridge health monitoring-based fatigue assessment.

**Keywords:** fatigue, finite element modeling, truck traffic loading, microscopic traffic simulation, cross-frame

## 1. Introduction

Fatigue is a common failure mode of steel bridges. About 80–90% of failures in steel structures are related to fatigue and fracture [1]. Despite the deterioration caused by environmental factors, the increasing traffic volume and weight pose a premier threat to steel highway bridges. The total number of truck passages in the 75 year life of a highway bridge could exceed 100 million [2]. With the aging of existing steel highway bridges and the accumulated damage under truck loading, the fatigue assessment for continuing service has become important for decision makings on the structure maintenance, component replacement, and other major retrofits.

Given the uncertainties of the complicated traffic loading and the complexity of the bridge structure, fatigue evaluation based on field measurements under actual traffic flow is recommended by many researchers. As the quality and quantity of the available long-term traffic monitoring data and information have been improved, a set of methodologies has been developed to obtain a more realistic vehicular live

load. The knowledge of actual traffic loading may reduce the uncertainty involved in the evaluation of the load-carrying capacity, estimation of the rate of deterioration, and prediction of remaining fatigue life. However, there are still some difficulties in field measurements. For example, some highway bridges are not accessible for field tests; the maintenance of monitoring system is difficult and costly, especially for long-term monitoring; some highway bridges will not even be considered for field tests with economic concerns.

The results of several NCHRP reports, written by Dr. John Fisher in 1970s, have confirmed that for welded details, fatigue life is primarily a function of stress range, detail category, and the number of applied cycles. The live load of a bridge includes static and dynamic parts while the early research and studies focused on the static portion. Schilling [3] and Raju et al. [4] suggested to improve the accuracy of the fatigue truck model by adjusting the fatigue truck axle weights in proportion to an equivalent total weight calculated from the specific site load distribution. The collected weigh station measurements, or data measured in stationary weight scales, were used by Nowak et al. [5] to determine the truck-load spectra for highway bridges on highways I-75 and I-94. Later, Laman and Nowak [6] developed a fatigue-load model from weigh station measurements and calculated the statistical parameters of stress for girder bridges. The results indicated that magnitude and frequency of truck load spectra are strongly site-specific and the live load stress spectra are strongly component-specific. With the advantage of weigh-in-motion (WIM) technology, Miao and Chan developed a methodology by using 10 year WIM data for deriving highway bridge live load models for short span bridges in Hong Kong [7]. NCHRP developed a set of protocols and methodologies for using available nation-wide, state-specific, or site-specific truck traffic data collected at different U.S. sites to obtain live load models for LRFD superstructure design, fatigue design, deck design, and design for overload permits [8].

In the early studies, it was commonly assumed that a certain percentage of the total weight was loaded on the front axle or rear axle for the magnitude and configuration. Further, there was no real traffic simulation considering the truck flow pattern. Bridge behavior simulations under truck loading were usually performed using the Monte Carlo method, which is a statistical projection approach with generic nature and does not consider any vehicle and driver behavior models when simulating truck traffic flow. In recent years, traffic flow simulation method has been applied to provide instantaneous information of individual vehicle by many researchers. Chen and Wu developed a general framework of modeling the live load from traffic for a long-span bridge by using the cellular automation (CA) traffic flow simulation technique. A typical four-lane long-span bridge was studied using the proposed method. Each lane was divided into cells with an equal length of 7.5 m. Three conditions, the free flow, the moderate flow, and the congested flow, were considered in the simulation. A simple comparison between the simulated static traffic load and the AASHTO LRFD HL-93 design load was conducted. The results showed that the HL-93 may be insufficient for the congested flow condition [9].

This research has developed a framework for the fatigue assessment of steel highway bridges based on simulated truck loading. The proposed methodology is implemented on a steel highway girder bridge on interstate 270 (I-270) over Middlebrook Road in Germantown, Maryland. With the help of the available long-term monitoring traffic data, truck loading was also obtained through the probability-based model. Then, the three-dimensional finite element (FE) global bridge models were studied subjected to the simulated truck loading. Meanwhile, the preliminary field test and the long-term monitoring test were also conducted. The FE models were calibrated with the collected field measurements through monitoring systems, and the simulated numerical structural responses were validated.

Lastly, this model has been used for identifying the cause of fatigue cracks reported in the biennial bridge inspection. Thus, the proposed methodology could be used to realistically simulate the fatigue behavior of steel highway bridges under current or future truck loading, to direct the experimental designs and instrumentation plans before performing experiments on laboratory or on site, and to better understand the fatigue mechanism and prevent the fatigue damage of steel highway bridges.

## 2. Fatigue cracks and bridge testing

### 2.1 Bridge introduction

The I-270 Bridge over Middlebrook road (MD Bridge No.15042) is a simple-span composite steel I-girder bridge with a span length of 140 ft. This bridge is comprised of two structures for the northbound (NB) and southbound (SB) roadways respectively, separated at the centerline. It carries three traffic lanes in the southbound and four traffic lanes in the northbound with equal lane widths of 12'-0".

The southbound superstructure provides a curb-to-curb roadway width of 61'-2" and consists of eight identical welded steel plate girders with a composite reinforced concrete deck constructed with shear connectors. The eight girders are equally spaced at 7'-11" and each girder has a constant web depth of 60" throughout the entire bridge. The northbound superstructure provides a curb-to-curb roadway width of 73'-1" and consists of nine identical welded steel plate girders with a composite reinforced concrete deck constructed with shear connector. The nine girders are equally spaced at 8'-5" and each girder has a constant web depth of 60" throughout the entire bridge. This bridge has a 76 degree parallel skew of its bearing lines (or 14 degree measured from normal). The cross-frames are inverted K-type braces with bottom chords only. All of them are parallel to the bearing lines. Girders of the southbound superstructure are numbered as G1 through G8 from the exterior to the centerline of the bridge. The cross section is depicted in **Figure 1**.

Designed in 1988, the I-270 Bridge over Middlebrook Road has been in-service for over 20 years. In addition to the deterioration caused by environmental factors, the bridge structure has also been subjected to increasing traffic volume and weight. Four fatigue cracks as marked on **Figure 2** were reported in the June 2011 Bridge Inspection Report, and all in the welded connection between the lower end of the cross frame (**Figure 3**) connection plate and the girder bottom flange of the southbound superstructure. **Figure 4(a)** shows one of the four crack locations at G3B2D3 (Girder 3 Bay 2 Diaphragm 3). Therefore, only the southbound superstructure will be discussed in the following sections. Most bridge components with fatigue cracks are repaired or replaced shortly after the crack is found in an inspection. However, since the crack on the I-270 Bridge was identified on a secondary bridge member,

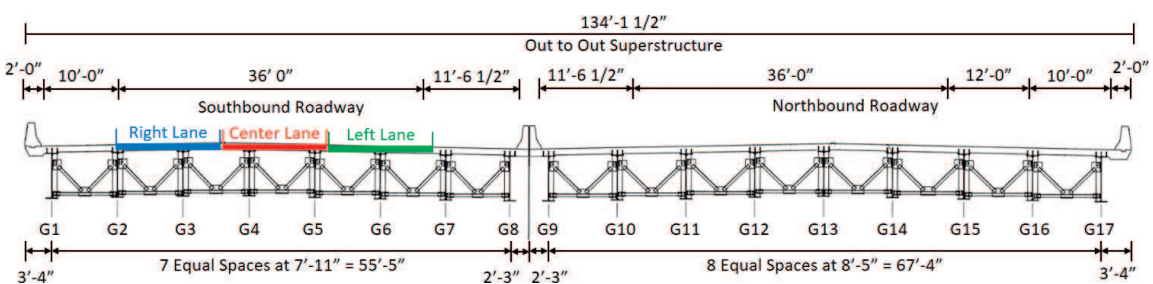


**Figure 1.**  
Cross section with lane positions.



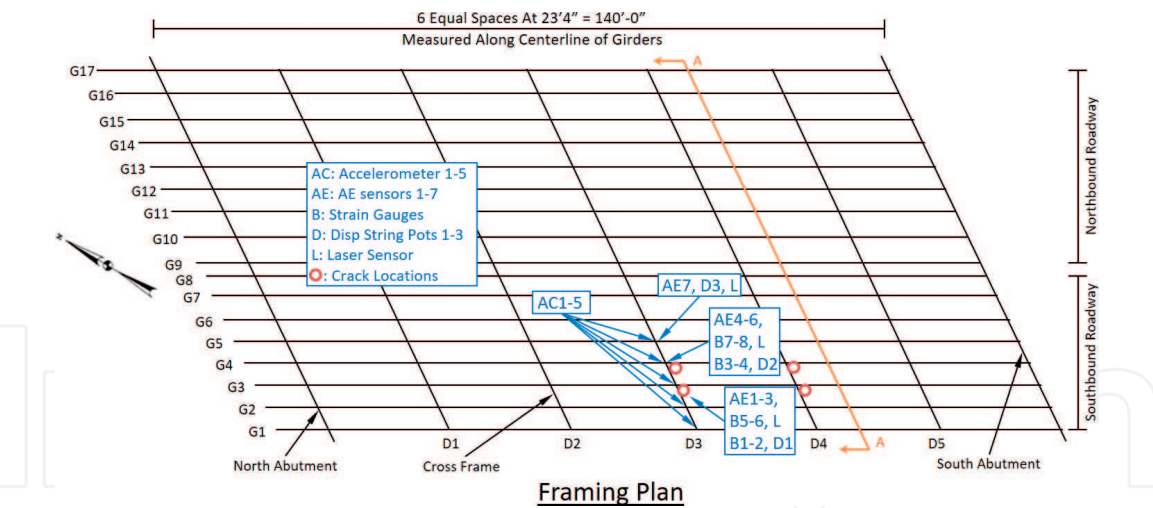


Figure 2.  
Crack locations and sensor placements on the framing plan.

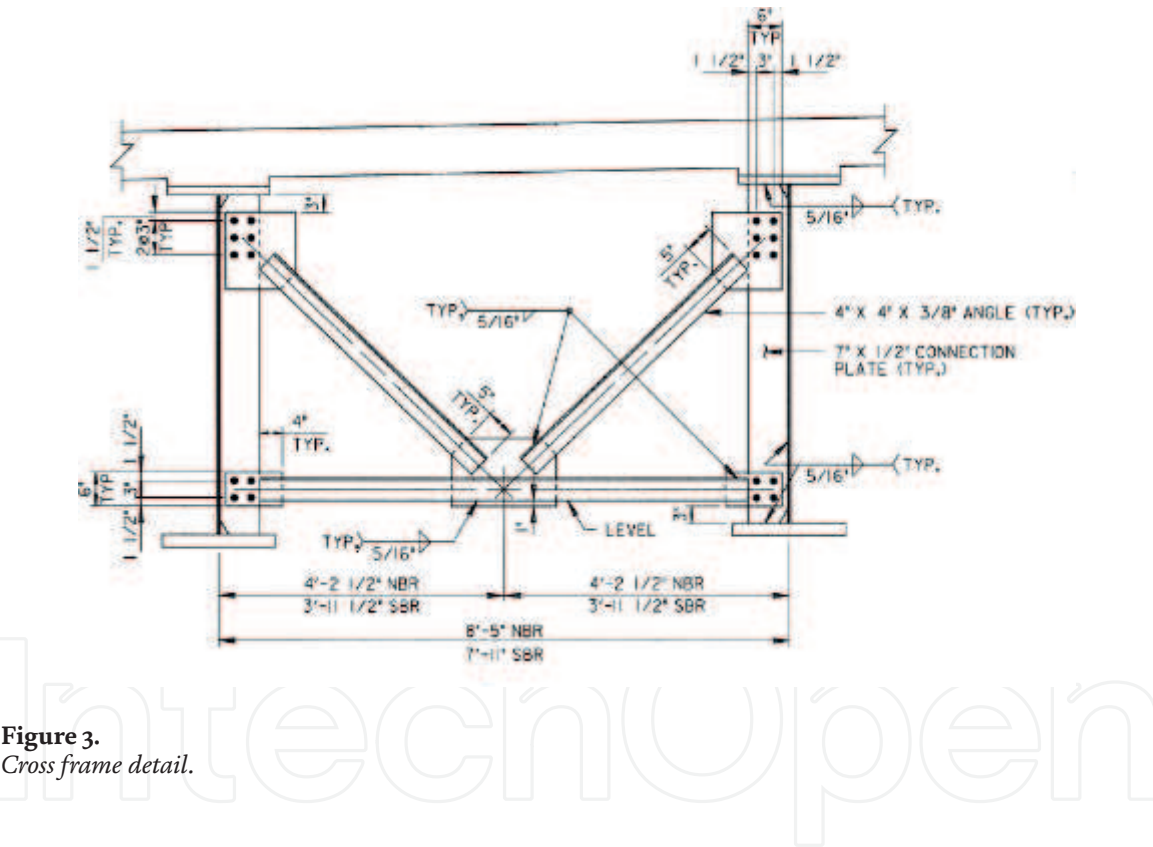


Figure 3.  
Cross frame detail.

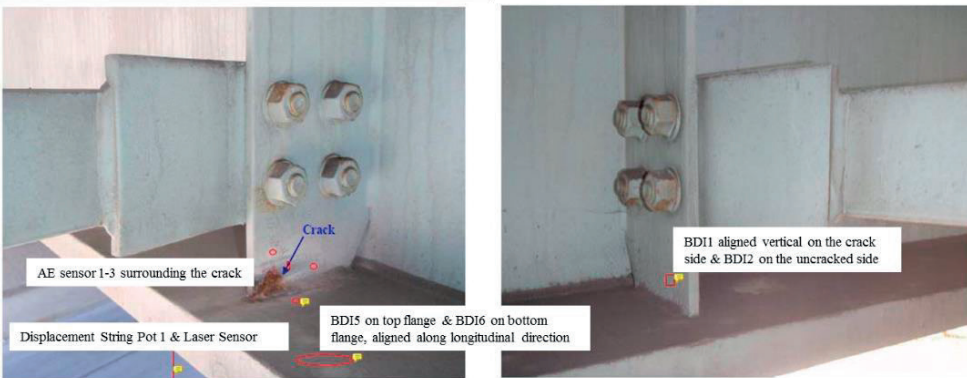


Figure 4.  
Crack locations and sensor placements: (a) details at G3B2D3 and (b) details at G3B3D3.

and delaying repair would not jeopardize the safety of drivers, this crack was selected for research purposes and long-term monitoring.

## 2.2 Field test and results

The field test of the I-270 Bridge was conducted through a Wireless Integrated Structural Health Monitoring System sponsored by the U.S. Department of Transportation, Office of the Assistant Secretary for Research and Technology (USDOT/OST-R). This smart bridge condition monitoring system, termed the ISHM system, features a number of technology innovations, including remote sensing capability, piezo paint acoustic emission sensors, wind and solar based energy harvesting devices to power the sensor network, high-speed wireless sensing ability and advanced data analysis methods for remaining life estimation of aging bridges. Through successful advancement and commercialization in the state-of-the-art technology of remote infrastructure sensing, the ISHM system is promising to reduce life cycle costs while significantly maintaining the sustainability of the highway infrastructure in the US.

### 2.2.1 Instrumentation plan

The main data acquisition systems used in this test consisted of a PXI-based data acquisition system by National Instruments, which was used for data collection by the BDI strain transducers, string pots and Acoustic Emission (AE) sensors, and a multi-channel data acquisition equipment CR5000 manufactured by Campbell Scientific, Inc., which was used for the extra BDI strain transducer. Types of sensors used in this project were: (1) piezoelectric paint AE sensors; (2) wireless accelerometers; (3) laser sensor; (4) ultrasonic distance sensors; (5) BDI strain transducers; and (6) string pots. Sensors were strategically placed where the cracks on the SB bridge were identified and their related strain, AE or supplemental data can be collected by the data acquisition system and later used for validating the FE models. The instrumentation plan is shown in **Figure 2**. Girder displacement and stress range records due to truck traffic were part of the field measurements in this study.

### 2.2.2 Vibration response

A total of four wireless accelerometers were used to monitor the vibration responses of the bridge. Wireless sensors were installed on four girders (Girders 2–5) and acceleration data were acquired at 100 Hz sampling rate synchronically. The acceleration data were used to provide modal frequency information that was used to calibrate the finite element model of the bridge. The fundamental frequency measured is 3.22 Hz, which was very close to the value of the first vertical mode from the finite element analysis of 3.24 Hz discussed in the following sections.

### 2.2.3 Bridge deflection

Both laser sensor and ultrasonic distance sensors were used to measure the dynamic deflection of the bridge. Only one laser sensor and one ultrasonic distance sensor were used each time. The measured deflection value from the laser sensor agreed well with the string pot, and its accuracy was also validated by the fundamental frequency indicated by fast Fourier transform (FFT) of the laser sensor measured deflection data. The measured maximum deflection of the I-270 bridge over Middlebrook Road under traffic loading is summarized in **Table 1**.

Girder number	3	4	5
Max D (in)	0.2598	0.2717	0.2480

**Table 1.**  
*Maximum deflections measured by laser sensor.*

2.2.4 Stress

Cracks occur in the direction perpendicular to the direction of principal tensile stress. To assess the driving force of the fatigue cracks in the connection welds, strain gages were placed vertically on the connection plate just beyond the tip of the existing crack. Strain gages were also placed longitudinally on the girder flanges to correlate with the occurrence of vehicular loads. For comparison with the results from analytical methods, field testing is applied as it is the most accurate approach since no assumptions need to be made for uncertainties in load distribution such as unintended composite action between structural components, contribution of nonstructural members, stiffness of various connections, and behavior of the concrete deck in tension. The actual strain histories experienced by bridge components are directly measured by strain gages at the areas of concern. The effects of varying vehicle weights and their random combinations in multiple lanes are also reflected in the measured strains.

BDI 1-4 strain transducers were placed on both sides of the connection plates while BDI 5-8 strain transducers were placed at the top and bottom flanges on Girders 3 and 4 (**Figure 2**). **Figure 5** shows the measured stresses on the flanges and connection plates, respectively. The maximum stress measured at the bottom flange was 1.604 ksi in tension for BDI 3215 on the bottom flange of Girder 3 due to regular traffic loading, which was very low comparatively. As for the connection plates, the maximum stresses were 16.18 ksi in tension for BDI 1641 on Girder 3 and 16.1 ksi in tension for BDI 1644 on Girder 4 (**Figure 5**).

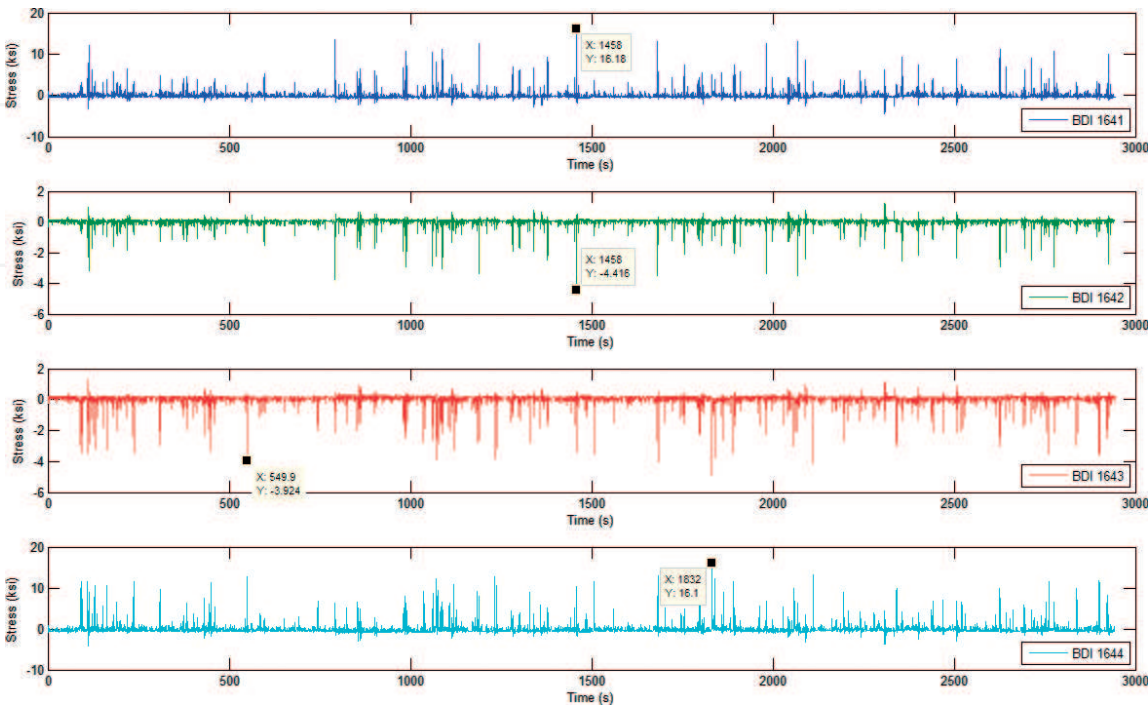


**Figure 5.**  
*BDI strain transducer measurements of connection plates and flanges (positive indicates compression; 1641 G3 cracked side; 1642 G3 uncracked side, 1643 G4 uncracked side and 1644 G4 cracked side).*



### 3. Finite element modeling

#### 3.1 Traffic loading

The traffic data that is used to simulate the traffic flow were the time-varying vehicle count data obtained from the Traffic Monitoring System Program (TMSP); operated and maintained by the Highway Information Services Division under Maryland Department of Transportation, State Highway Administration (MDSHA) [10]. The TMSP has been responsible for the collection, processing, analysis, and management of Maryland highway traffic data since 1997. Under this program, MDSHA has implemented 79 permanent continuous automatic traffic recorders (ATRs) counting traffic continuously throughout the year, and over 3800 short-term (48 hour) program count locations throughout the state, with data taken during the week on either Tuesday and Wednesday or Wednesday and Thursday to reflect typical weekday travel patterns. These monitoring systems are installed across Maryland and monitor most of the arterials, freeways, and interstates. **Figure 6** displays the location of several ATRs on I-270.

The TMSP has also created an Internet Traffic Monitoring System (I-TMS) that provides access to detailed traffic count data. On the I-TMS, the user can select an individual location to view reports (class, volume, lane distribution, etc.). Based on the hourly traffic volume, one typical day was divided into four different time periods: midnight, early morning and night, morning peak hour, and noon to evening, as shown in **Table 2**. The durations for these four time periods are 5, 5, 5, 9 hours, respectively. The average hourly volume varied from 505 to 4215, and the truck percentage also varied from 10.39 to 20.10%. Lane distribution of I-270 Bridge over Middlebrook Road is shown in **Table 3**. The main purpose of this time division is to realistically simulate the major characteristics of the traffic flow for each time period.

Following the specifications in the Guide Specifications for Fatigue Evaluation of Existing Steel Bridges (1989), weigh station measurements were collected at Hyattstown Weigh Station. From these measurements, a gross-weights histogram was obtained for the truck traffic, which was used to calculate the effective gross weight of the fatigue truck. The Hyattstown Weigh and Inspection Station is located approximately 10 miles north of I-270 Bridge over Middlebrook Road,

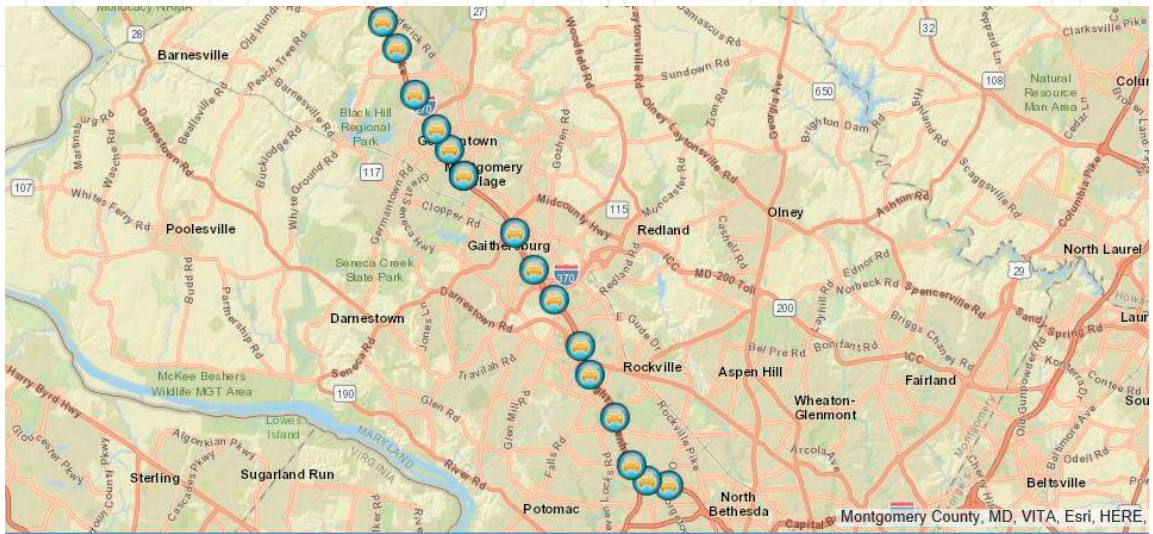


**Figure 6.**  
*Observation points on I-270 in Montgomery County.*



Time period	Time	Average total volume (no. of vehicles per hour)	Passenger car (no. of vehicles per hour)	Truck by axle number (no. of vehicles per hour)					Truck percentage
				2	3	4	5	6	
Midnight	23:00–24:00 0:00–3:00 (5 hours)	505	403	25	2	3	69	3	20.10%
Early morning and night	4:00–5:00 19:00–23:00 (5 hours)	1934	1712	55	4	7	150	6	11.40%
Moring peak	5:00–10:00 (5 hours)	4215	3759	113	7	14	310	12	10.82%
Noon to evening	10:00–19:00 (9 hours)	3021	2707	78	5	9	213	8	10.39%

**Table 2.**  
*Traffic condition under different time period.*

Vehicle type	Left lane (%)	Middle lane (%)	Right lane (%)
Total (passage car and truck)	31.87	30.62	37.51
Truck	1.45	44.84	53.71

**Table 3.**  
*Lane distribution of one typical day.*

along Interstate 270 (I-270). Around 2200 samples during 1 year were chosen as the database to generate the truck weight and configuration. The measured data were filtered before the statistical analyses were made, where five samples were deleted. All the trucks were cataloged into seven classes based the number of axles (**Figure 7**). It is clear that 2-axle trucks and 5-axle trucks were the majority, which occupies about 24.87 and 67.99%, respectively. The 3-axle trucks, 4-axle trucks and the heaviest 6-axle trucks and over accounted for 1.61, 2.98 and 2.55%, respectively, which adds up to 7.14% in total.

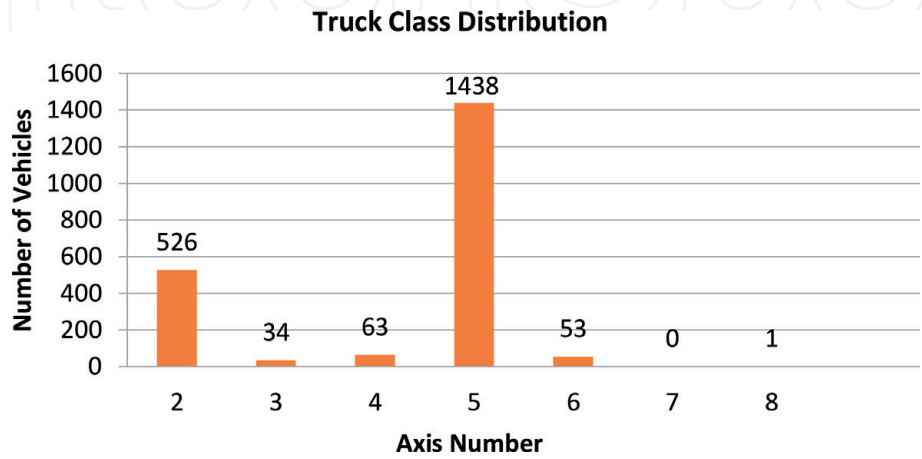


**Figure 7.**  
*Truck class distribution.*

Because of the limitation of the traffic simulation software CORSIM, only three different types of trucks can be defined during traffic simulation: the small truck, the medium truck, and the large truck. Since 2-axle trucks and 5-axle trucks were the majority, the small truck was defined to consist 2-axle trucks and 3-axle trucks, and the medium truck to include 4-axle trucks and 5-axle trucks. For safety consideration, the heaviest 6-axle trucks and over were also considered as the third type, although it only takes a very small percentage.

The effective gross weight of the fatigue truck was computed from Eq. (1)

$$W = \left(\sum f_i W_i^3\right)^{1/3} \tag{1}$$

where  $f_i$  is the fraction of gross weights within an interval and  $W_i$  is the midwidth of the interval. The gross weight was distributed to axles in accordance with the site data. The final fatigue truck configurations were shown in **Figure 8**.

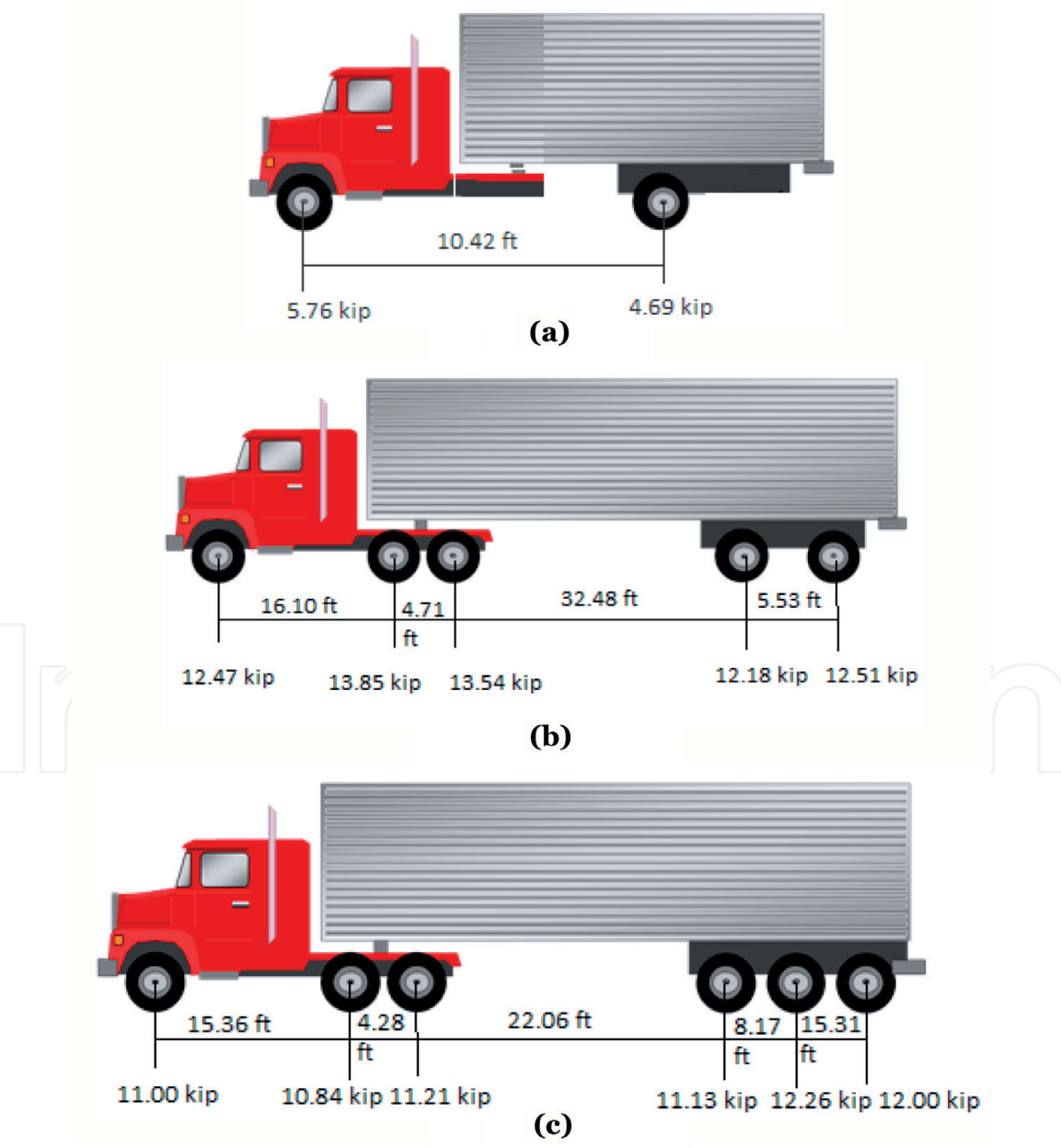


**Figure 8.**  
Fatigue truck configurations: (a) small truck; (b) medium truck; and (c) large truck.

As an intercorrelated component of a whole transportation network, the actual traffic flow through a bridge is affected by the traffic on the connecting roadway segments. Therefore, to realistically capture the major characteristics of the traffic flow, a road network system consisting of the bridge, highway, and two neighboring ramps was studied in the present work. The detailed procedure is summarized in four steps:

1. Build the simulation network (**Figure 9**) in TSIS 5.1 [11] around the I-270 over Middlebrook Road based on the background map obtained from Google Maps. The background map is adjusted to the correct scale, and the simulation network is drawn along the real roadway segment. The network contained the mainline of I-270 and adjacent on-ramps of the bridge in the study. Since the focus is on the southbound of the bridge, the network only contains one-way southbound link. The simulation time is set to be 1 hour.
2. Use the time varying vehicle count data collected from nearby detectors, which were placed on the I-TMS website, and combine with the weigh station measurements collected from the Hyattstown southbound station as the input data for the simulation model. The truck count data from the vehicle count report are converted to truck percentage (truck count/total vehicle count) as the input for CORSIM simulation.
3. Set three different types of trucks corresponding to fatigue trucks generated in the last section. Install three loop detectors at the bridge in the created simulation network, one for each lane to record the speed, type, and passage time of the detected vehicles.

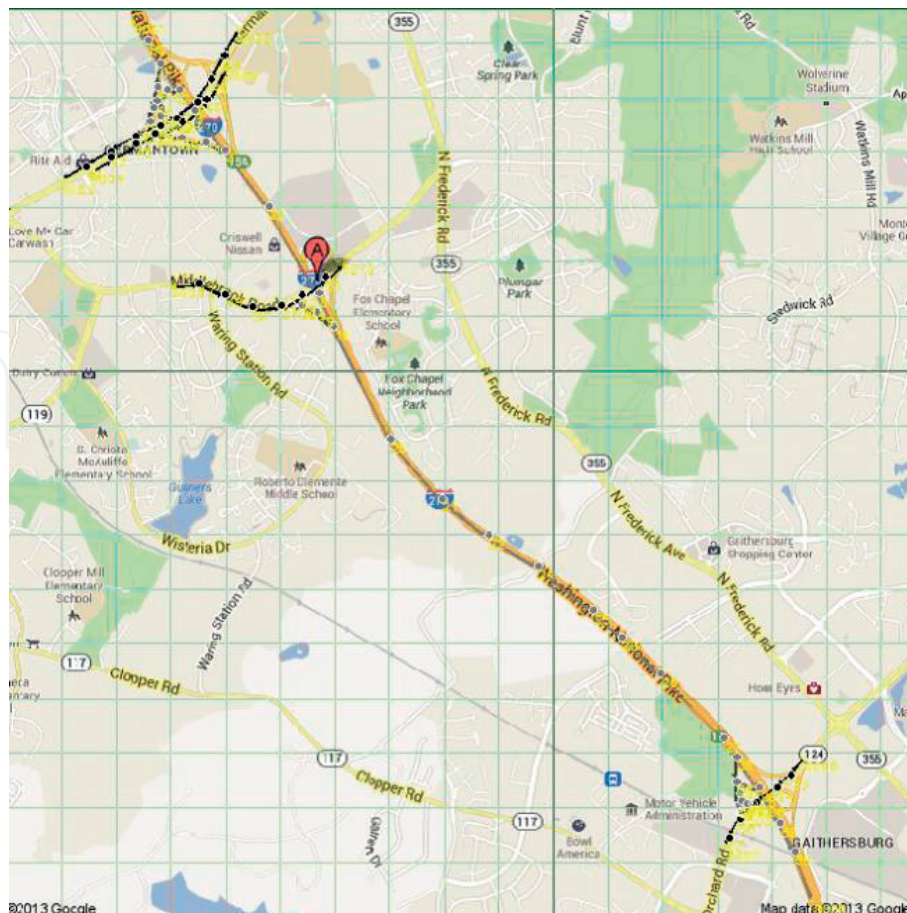


**Figure 9.**  
Traffic simulation network.



4. After the simulation network is created, the traffic demand is input and calibrated, and the detectors are installed, the CORSIM simulation can begin. The simulation provides the following meaningful results for the analysis. First, it records the animation of the simulation, which is used to observe the passage time of the trucks. Second, it provides text output including the volume and speed statistics by each interval (set to be 1 s here). Combining the above two outputs, the passage time and the lane occurred and speed of the truck could be successfully matched.

The results (**Table 4**) could provide vehicle position and speed at each time step of the simulation. It was found from the results that the 20 min simulation period currently used can lead to stable pattern and matched field monitoring results. Details of the field monitoring are reported in a separate companion paper, “*Integrating Bridge Management Systems with Fatigue Damage Assessments.*”

3.2 Bridge global model

To investigate the fatigue performance of the bridge, a three-dimensional finite element model was developed for linear-elastic structural analysis using the CSiBridge [12], as depicted in **Figure 10**. The model of the southbound superstructure consisted eight I-girders. The concrete deck, the eight I-girders, and connection plates which connected cross-frames to the girders were modeled by shell elements, while all the cross-frames were modeled by spatial frames along their center-of-gravity. Special link members were defined to connect girder elements and concrete deck elements at the actual spatial points where these members intersect. The translations in the x-, y-, z-directions were fixed at the abutments to represent the actual characteristics of support and continuity. It is complicated to establish a comprehensive finite element model of a large practical structure for fatigue damage analysis, since the finite element model should

Time periods	CORSIM		
	Average speed (mph)	Number	Average headway (s)
Midnight	53.69	32	37.5
Early morning and night	52.94	78	15.38
Morning peak	35.45	165	7.27
Noon to evening	42.07	98	12.24

**Table 4.**  
CORSIM simulation results.

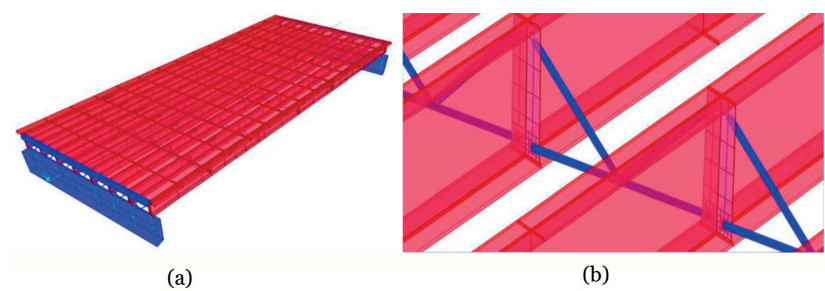


**Figure 10.**  
Finite element model of I-270 Bridge in CSiBridge: (a) isometric view of FEM for I-270 Bridge and (b) zoom-in view (refined meshing around the welds).

embody the sectional properties of structural members (e.g., the weld between two members). In addition, fatigue damage is a local failure mode and often occurs around welded regions. Therefore, a global model with refined meshing around the welded connection between the connection plates and the bottom flanges was constructed for analysis.

### 3.3 Convergence test

The accuracy of a finite element analysis depends on the mesh size of the elements; the smaller the size of the elements, the greater the accuracy of the analysis. However, the desire for increased calculation accuracy can significantly increase the computational time. Therefore, in finite element analysis, a convergence test is used to determine appropriate mesh size for a model without increasing the computation time. The measurement of a finite element model's mesh size depends on the purpose of the model. Since this bridge model is to investigate the vertical stress or shear stress in the cracked connection weld, it needs to have a very fine mesh in the connection area but needs to also transit gradually to coarser meshes because otherwise the model would become unnecessarily too large. A more uniform mesh may then be used along the rest of the bridge length for all the girders. However, there are multiple parameters related to the accuracy of a two-dimensional or three-dimensional finite element model, including the dimensions and aspect ratios of the elements for the girder top flange, bottom flange, and web, as well as the bridge deck.

To simplify the convergence test for these finite element models of the I-270 Bridge over Middlebrook Road, a consistent refined mesh around the weld region was employed in all the models, and the maximum element size was used to control the uniform mesh along the bridge longitudinal length for all the girders and the deck. The determination of the first natural frequency was used as the measurement during the convergence test. As the maximum mesh size changed from 1000 in to 0.5 in, the results of the first natural frequency gradually increased from 2 to 3.20 Hz. The results of the first natural frequency were all beyond 3 Hz when the maximum mesh size of the finite element models was smaller than 200 in, which means that the error rate of the first natural frequency was under 6.25%. When the maximum mesh size was equal to or less than 50 in, the results of the first natural frequency were accurate enough with an error rate less than 2%, and were therefore used as the basis for the selection of an accurate finite element mesh in CSiBridge.

### 3.4 Modal analysis

Modal analysis is used to determine the vibration modes of a structure. These modes are useful to understand the behavior of the structure. They can also be used as the basis for modal superposition in response-spectrum and modal time-history load cases. An eigenvector analysis was used to determine the undamped free-vibration mode shapes and frequencies of the system.

The first six mode shapes of torsion, vertical and lateral modes are shown in **Figure 11**. To validate the finite element models, experimental data from the field test and numerical results from CSiBridge were studied. In the numerical study, the bridge was only subjected to dead load. The results obtained from the finite element model and field measurements were compared, and the differences of most of the compared frequencies were less than 6%, which was considered acceptable for the finite element analysis. All the mode shapes matched well with each other. Therefore, the CSiBridge model was considered reasonably accurate for the purposes of this study.

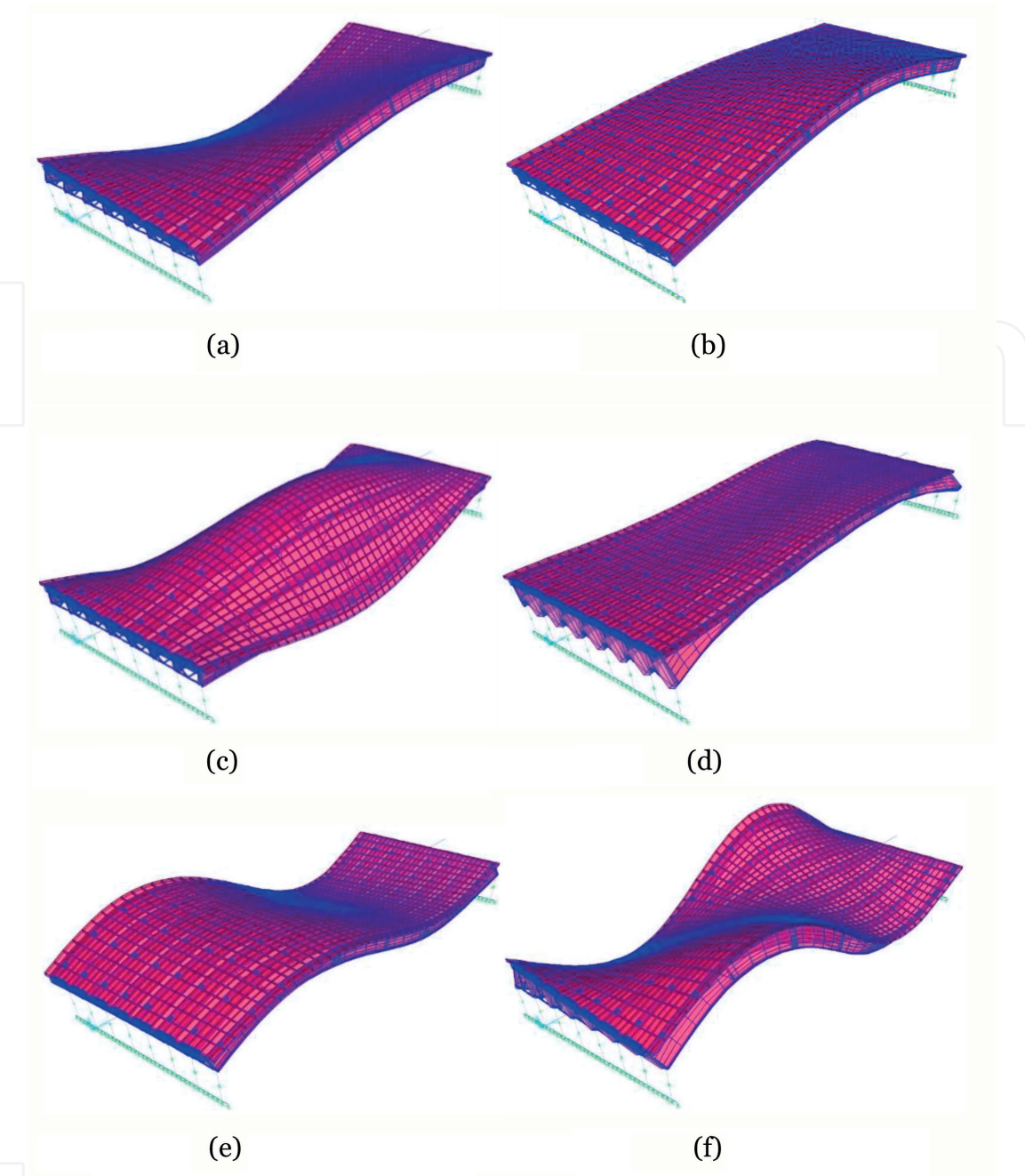


**Figure 11.** Mode shapes of I-270 Bridge over Middlebrook Road in CSiBridge: (a) mode shape 1 (first torsion), (b) mode shape 2 (first vertical), (c) mode shape 3 (second torsion), (d) mode shape 4 (first lateral), (e) mode shape 5 (second vertical), and (f) mode shape 6 (third torsion).

### 3.5 Stresses by simulation

Possible driving forces for the fatigue cracks shown in **Figure 4** are vertical tensile stress, horizontal shear stress, or the principal tensile stress due to their combined actions along the connection welds. Live load induced stresses from the welded connections between the cross-frame connection plates and the girder bottom flanges were extracted in the refined portion of the finite element models. A total of four different traffic loading cases obtained from the traffic simulation were studied as described below and the key results were summarized in **Table 5**. For all the four cases analyzed, the longitudinal positions of trucks remained the same as for the previous deflection studies.



Time period	Max vertical stress	Max shear stress	Max principal stress
Midnight	6.665	2.165	7.629
Early morning and night	7.586	2.563	8.70
Morning peak	12.94	4.327	14.84
Noon to evening	7.905	2.664	9.061

**Table 5.**  
*Stresses in cross frame connection plate-to-girder bottom flange connections at G3 without dynamic impact (FE results) (ksi).*

There were many live load cases that could have produced significant tensile stresses in the connections of concern. The simulated truck loading contained most of the possible truck loading patterns. Magnitudes of tensile stresses in the connection plates depend on the magnitudes and positions of the wheel loads of crossing vehicles. The stresses listed in **Table 5** are for illustration and are taken from the connection plates at Girder 3 for the four different time periods. A comparison of live load cases for the four different time periods suggest that live loads during morning peak may have caused the highest tensile stress of 12.94 ksi in the connection of concern. All the shear stresses in the connection welds were much lower than the vertical stresses at the same spot during each time period. Considering a factor of dynamic load allowance, the dynamic maximum vertical stress was 16.822 ksi, which perfectly matched with the field measurements.

## 4. Cause of fatigue cracks

### 4.1 Connection plate configuration

The results of the finite element analysis were verified and validated with the field test data; all the cracks were located on the western sides of the connection plates. The vertical stress near the welded edges of the connection plates followed the same pattern; the western sides of the connection plates were under tension; and the eastern sides of the connection plates were under compression. To further discuss the cause of this phenomenon, a series of controlled FEM tests were established for the comparison study.

According to the design drawings and the existing bridge construction, cross-frame connection plates and bearing stiffeners are normal to the girders and connection plates connecting the cross-frames are bent. Therefore, for the original FE model, all the connection plates were normal (90°) to the girders and the cross-frames are parallel to the two abutments with a skew angel of 76°. For the controlled model, all the connection plates were parallel to the cross frames with the same skew angel of 76 degree (**Figure 12**).

### 4.2 Bracing system configuration

The K-type bracing system was modeled for studying the influence of the bracing system configuration on the stress distribution in the connection plates. The K-type cross-frame without top chord was modeled in the original FE model, while the K-type cross-frame with top chord was modeled in the controlled

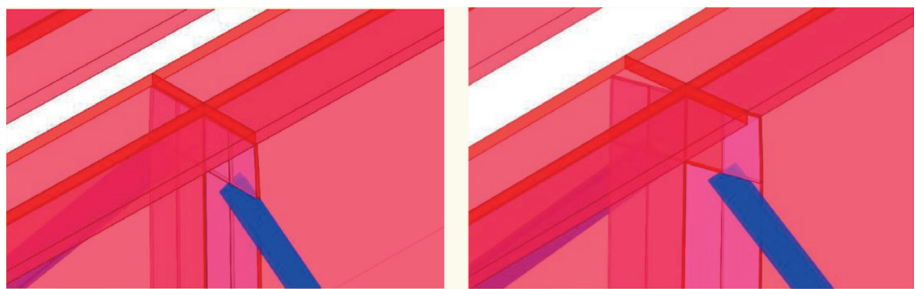


**Figure 12.**  
*Skewed (right) and non-skewed (left) connection plates.*

model. The cross section of the diagonal and bottom chords was employed for the additional top chords (**Figure 13**). All the models were subjected to the same live load case. The live load case was defined as an HS20 truck in the right traffic lane passing across the bridge from north to south at the speed limit of 55 mph. The vertical stress at the crack location (Girder 3 Diaphragm 3) and the axial forces in the top chord located at Diaphragm 3 Bay 2, directly connecting with the crack side, were analyzed and are shown in **Table 6**. Maximum vertical stresses in the model with the non-skewed connection plates were much higher than the stresses in the model with the skewed connection plates. The maximum axial forces in the models during the load time history analysis were quite small; the values were only 3.47 and 1.12 kip. The values of maximum vertical stresses did not change much due to the addition of a top chord. It demonstrates that the connection plate configuration has a significant influence on the stress distribution in the connection plates, while

Connection plates configuration	Bracing system configuration	Maximum axial force (kip)	Maximum vertical stress of crack location (ksi)
Non-skewed connection plats	K-frame without top chord	—	13.50
	K-frame with top chord	3.47	12.66
Skewed connection plats	K-frame without top chord	—	0.33
	K-frame with top chord	1.12	0.30

**Table 6.**  
*Maximum vertical stress and axial force through simulated numerical analyses.*

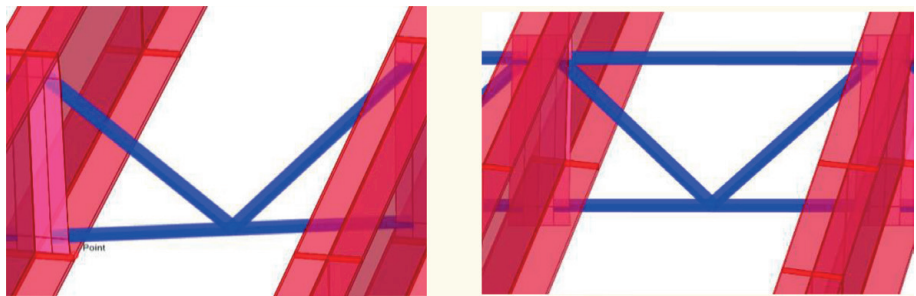


**Figure 13.**  
*K-frame without top chord (left) and K-frame with top chord (right).*

the top chord of K-type bracing plays a negligible role in this situation. Further, the results showed that X-type or K-type bracing made no difference on the vertical stress at the crack location.

The measured high vertical tensile stress around the connection plate welds was proven caused by the configuration of the connection plates instead of the configuration of the cross-frames. The connection plates, which were bent to be parallel to the skewed abutment, induced torsion in the connection plate welds. Differential displacements between the girders caused one diagonal cross frame to be in tension and the other diagonal to be in compression. Measured vertical tensile stresses from field tests up to 16.1 ksi in the connection plate explains why fatigue cracks have occurred at their connections to the girder bottom flange. Girders 3 and 4 are located under the slow-moving lane which most heavy trucks are using while Girders 1 and 2 support a shoulder and thus larger differential deflections typically occur between Girders 2 and 3 (with up to 0.5" to 0.75" vertical deflections due to observed live load). The connection plate configuration is a key factor in the stress distribution that results in the connection plates.

## **5. Conclusions**

The passage of trucks on the bridge deck can cause vertical tensile stresses in the welded connections between cross-frame connection plates and girder bottom flanges. These stresses were highest at the outer edge of the connection plate where all the existing four fatigue cracks on the I-270 Bridge over Middlebrook Road were located. Girder 4 located at the center left of the middle traffic lane, and Girder 3 located at the center right of the right traffic lane, are the most critical locations for the bridge deflections and the resulting stresses.

The live load-induced stresses in the connection plates were localized around the welded connections and would not be anticipated to spread from the bottom to the top of connection plates. At the same face of the connection plate, both tensile and compressive stresses were observed at the symmetric positions around the girder web. The cracked side of the connection plates was always under tensile stress, while the uncracked side was always under compressive stress during each time period. At the same location of the cracked side, the north face and the south face sustained the same stresses, (although opposite directions). It was proved that the high vertical tensile stress around the connection plate welds was caused by the configuration of the connection plates instead of by the configuration of the cross-frames. The connection plates, which were bent to be parallel to the skewed abutment, induced torsion in the connection plate welds. The connection plate configuration is a key factor in the stress distribution that results in the connection plates.

Different from the explicit equation-based method, the proposed approach combines a comprehensive traffic loading model, which includes information on vehicle types, axle weights, axle spacing, and the lane occupation, and a detailed 3D FE model, which enables fatigue analysis on unreachable or complicated details where complex stress conditions may exist. The proposed approach may be used as a tool accompanying a monitoring program to find the stresses in unmonitored details or to reduce the frequency of structural health monitoring resulting in lower costs in fatigue assessment. In such case, the proposed approach also provides a tool to predict the fatigue reliabilities of these hard-to-reach details. When combined with the fracture damage mechanics, the proposed approach can help understand the accumulation of fatigue damage and crack propagation.



## Acknowledgements

This work was partially sponsored by the US Department of Transportation's Office of the Assistant Secretary for Research and Technology (USDOT/OST-R) under The Commercial Remote Sensing and Spatial Information (CRS&SI) Technologies Program. This support is acknowledged and greatly appreciated.

## Author details

Gengwen Zhao<sup>1</sup>, Chung C. Fu<sup>2\*</sup>, Yang Lu<sup>3</sup> and Timothy Saad<sup>2</sup>

<sup>1</sup> Virginia Department of Transportation, Richmond, VA, USA

<sup>2</sup> The Bridge Engineering Software and Technology (BEST) Center, Department of Civil and Environmental Engineering, University of Maryland, College Park, MD, USA

<sup>3</sup> Asian Development Bank, Mandaluyong, Metro Manila, Philippines

\*Address all correspondence to: [ccfu@umd.edu](mailto:ccfu@umd.edu)

## IntechOpen

© 2018 The Author(s). Licensee IntechOpen. This chapter is distributed under the terms of the Creative Commons Attribution License (<http://creativecommons.org/licenses/by/3.0>), which permits unrestricted use, distribution, and reproduction in any medium, provided the original work is properly cited. 

## References

- [1] Banjara NK, Sasma S. Evaluation of fatigue remaining life of typical steel plate girder bridge under railway loading. *Structural Longevity*. 2013;**10**:151-166
- [2] AASHTO. Guide Specifications for Fatigue Evaluation of Existing Steel Bridges. Washington, D.C: American Association of State Highway and Transportation Officials; 1990
- [3] Schilling CG. Stress cycles for fatigue design of steel bridges. *Journal of Structural Engineering*. 1984;**110**(6):1222-1234
- [4] Raju S, Moses F, Schilling C. Reliability calibration of fatigue evaluation and design procedures. *Journal of Structural Engineering*. 1990;**116**(5):1356-1369
- [5] Nowak AS, Nassif H, DeFrain L. Effect of truck loads on bridges. *Journal of Transportation Engineering*. 1993;**119**:853-867
- [6] Laman JA, Nowak AS. Fatigue-load models for girder bridges. *Journal of Structural Engineering*. 1996;**122**:726-733
- [7] Miao TJ, Chan THT. Bridge live load models from WIM data. *Engineering Structures*. 2002;**24**:1071-1084
- [8] NCHRP. Protocols for Collecting and using Traffic Data in Bridge Design. Washington, D.C: Transportation Research Board; 2011
- [9] Chen S, Jun W. Dynamic performance simulation of long-span bridge under combined loads of stochastic traffic and wind. *Journal of Bridge Engineering*. 2010;**15**:219-230
- [10] Internet Traffic Monitoring System. Maryland Department of Transportation State Highway Administration. Available from: [http://maps.roads.maryland.gov/itms\\_public](http://maps.roads.maryland.gov/itms_public). Accessed Jul. 29, 2015
- [11] ITT Industries, Inc., Systems Division: ATMS R&D and Systems Engineering Program Team; Colorado Springs, CO 80935-5012
- [12] CSiBridge. Integrated 3D Bridge Design Software. Berkeley, CA: Computer and Structures, Inc; 2010